Biomineralization

DOI: 10.1002/anie.201205336

Guanine-Based Photonic Crystals in Fish Scales Form from an Amorphous Precursor**

*Dvir Gur, Yael Politi, Berta Sivan, Peter Fratzl, Steve Weiner, and Lia Addadi**

A widespread material used by animals for producing structural colors is anhydrous guanine.[1] A relatively well studied system is the anhydrous guanine crystal arrays that are responsible for the metallic luster of many fish,[2,3] providing them with camouflage from a wide range of angles.[1,2d,4] Guanine may be the material of choice for this function because it is readily available in the cells as a nitrogenous metabolite, and anhydrous guanine has a very high refractive index, 1.83 in the reflecting direction.[1] The fish control the crystal orientation and morphology, including forming the crystals as thin plates that expose the high refractive-index plane.[3]

Many biological minerals crystallize through a transient disordered phase rather than directly from saturated solutions.[5] One advantage to this is that biomineralization processes often include molding the crystals into specific shapes. This molding process can be performed more easily using a disordered phase rather than a crystal, since crystals prefer to express specific shapes that reflect their atomic order.[6] After molding, the disordered phase is induced to crystallize.

To date, the disordered precursor phases used in biology are all ionic materials that transform into ionic crystals. There are in vitro studies of organic crystals that form by way of a disordered precursor phase.[7] Herein, we show that the crystals of anhydrous guanine in the scales of the Japanese Koi fish (*Cyprinus carpio*) form by way of a disordered guanine precursor phase. In Japanese Koi fish, the guanine crystals form inside specialized cells called iridophores (or guanophores) that are located beneath the mineralized scales and adjacent to the muscular layer.[2c,8] The anhydrous guanine crystals are part of a multilayer array composed of alternating layers of high refractive-index anhydrous guanine and low refractive-index cytoplasm (Figure 1 and Figure 2). This multilayer array interacts with incident light through constructive and destructive interference to produce a mirror-like sheen. Since the early studies of Fox, and Denton and Land,[2b,c,9] it is known that the guanine crystals form inside so-called membrane-bound crystal chambers (Figure 2a). The anhydrous guanine crystals from the Koi fish, as well as from a variety of organisms, including silver colored spiders,[3,8] all display an exceptional structure–morphology relation, as the direction expected to exhibit the highest growth rate, based on the crystal structure, is in fact the slowest direction of crystal growth. The expected theoretical morphology is indeed observed in some white spiders and in crystals grown from water.[3,8] The silver spiders produce a relatively thick (approximately 70 nm) layer of guanine, which contains stable amorphous guanine sandwiched between two 20 nm thick anhydrous guanine crystals. In contrast, the guanine

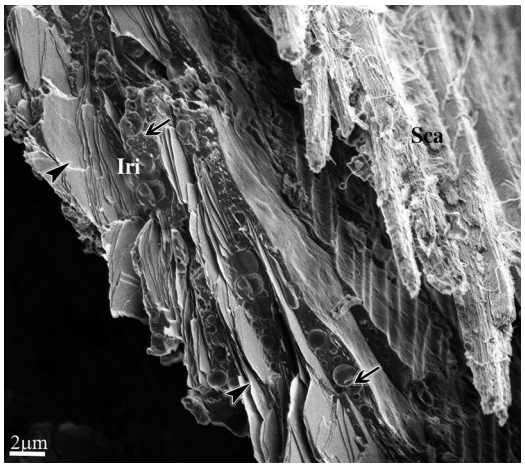

Figure 1. Gin rin Koi skin showing layers of iridophore cells (Iri) containing guanine crystals aligned in the plane of the scale (Sca) obtained by cryo-SEM. The scale is composed mainly of a mineralized collagen matrix. The black arrows point to thick layers of cytoplasm between the guanine crystal stacks and the outer membrane of the cell. The black arrowheads point to crystal stacks composed of alternating layers of guanine crystals and thin cytoplasm layers.

[*] D. Gur, Prof. S. Weiner, Prof. L. Addadi
Department of Structural Biology
Weizmann Institute of Science, Rehovot, 76100 (Israel)
E-mail: lia.addadi@weizmann.ac.il
Dr. Y. Politi, Prof. P. Fratzl
Department of Biomaterials, Max Planck Institute of Colloids and Interfaces, 14424 Potsdam (Germany)
Prof. B. Sivan
Department of Animal Sciences, Faculty of Agriculture
Hebrew University, Rehovot 76100 (Israel)

[**] We thank Dr. S. Siegel, Dr. C. Li and Dr. I. Zizak for their invaluable help in the μ-Spot X-ray diffraction studies. We thank the Mag Noi company from Kibbutz Gan Shmuel Israel, for supplying the fish. X-ray studies were conducted at the μ-Spot beamline of the BESSY II synchrotron radiation facility, which is part of the Helmholtz-Zentrum Berlin für Materialien und Energie, and received funding from the European Community's Seventh Framework Programme (FP7/2007-2013) under grant agreement no. 226716. The research was supported by a German Research Foundation grant, within the framework of the Deutsch-Israelische Projektkooperation DIP. L.A. is the incumbent of the Dorothy and Patrick Gorman Professorial Chair of Biological Ultrastructure, and S.W. of the Dr. Trude Burchardt Professorial Chair of Structural Biology.

Supporting information for this article (experimental details) is available on the WWW under http://dx.doi.org/10.1002/anie.201205336.

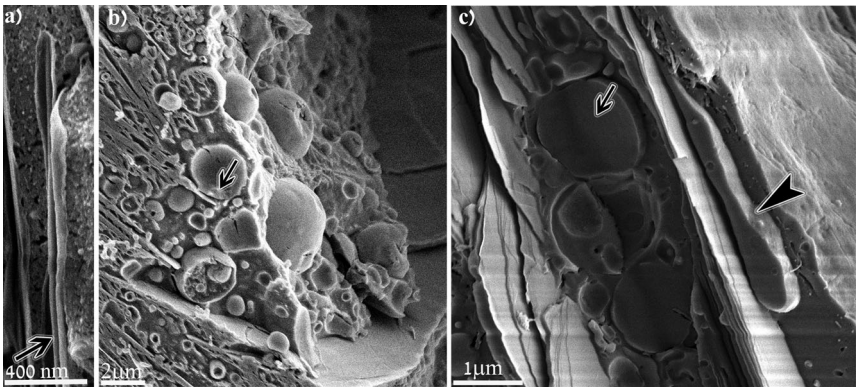

Figure 2. Iridophore cells containing intracellular guanine crystals: a) guanine crystal (black arrow) engulfed by a lipid membrane, called a crystal chamber; b,c) the iridophores contain vesicles filled with a dense material (black arrows). Even when fractured, the vesicles are much more resistant to water sublimation than the surrounding cytoplasm, indicating that they contain a denser material. In c) a vesicle close to the last layer of crystals appears to be elongated in the direction of the oriented crystal stacks (arrowhead). Cryo-SEM micrographs: a,c) were obtained after freeze fracture and b) after cryo-sectioning.

crystals in the Koi are composed of only one phase of guanine, namely anhydrous guanine (Supporting Information, Figure 1S).[3,8]

We used cryo-SEM imaging of untreated Koi fish skin and scales to study the tissue under hydrated conditions. The cytoplasm layers between the crystals are packed with vesicles 1–2 μm in diameter (Figure 2b,c). The cryo-SEM sample preparation procedure requires water to be sublimated from the freshly made fracture, to gain sufficient contrast for imaging (for experimental details see the Supporting Information). The material contained within the vesicles was not etched as much as the surrounding cytoplasm. Even when the vesicles were opened during the fracturing or sectioning process, their contents remained solid despite the intense etching (Figure 2b,c).

Furthermore, when examining the specimen under the electron beam, the vesicle exhibited much more resistance to beam damage than the surrounding cytoplasm. These two observations suggest that the material inside the vesicles is quite different from the surrounding cytoplasm, which consists mostly of water. Some of the vesicles that contained this material were elongated in the direction of the ordered crystal stack (Figure 2c). These vesicles were usually adjacent to the last formed layer of anhydrous guanine crystals.

Micro-spot X-ray diffraction[5c] was used to map the cross-sections of freshly extracted scales with the attached skin. We examined either fixed or frozen scales using the line (7T-WLS/1-μSpot) at the BESSY II synchrotron, Berlin (for experimental details see the Supporting Information). The samples were kept hydrated prior to the X-ray experiment, but during the experiment the wet cross-sections were exposed to air and thus partially dried.

X-ray fluorescence mapping of the calcium content of the scale cross-section (Figure 3a) allowed us to determine where to map the scale section. The measurements were made at 10 μm intervals using a beam 10 μm in diameter. The X-ray diffraction patterns (Figure 3b) were integrated into 2D plots and analyzed (Figure 4-1). Diffraction patterns collected in different areas on the scale showed different crystalline phases. Integrated diffraction patterns (Figure 4-1) from areas A, B, and C in the scale, correspond to positions A, B, and C in the Ca X-ray fluorescence map (Figure 3a). The peaks at 3.44 Å and at 2.77–3.22 Å correspond to the (002), (112), (211), (210), and (102) reflections of hydroxyapatite from the mineralized collagen part of the scale (area C). The peaks at 3.22, 6.22, and 7.82 Å correspond to the (102), (012), and (011) reflections of anhydrous guanine, respectively. The diffraction pattern of anhydrous guanine has a preferred orientation, which is in agreement with the {102} plate morphology of the biogenic anhydrous guanine crystals being oriented roughly parallel to the scale (Figure 1). In addition to the expected

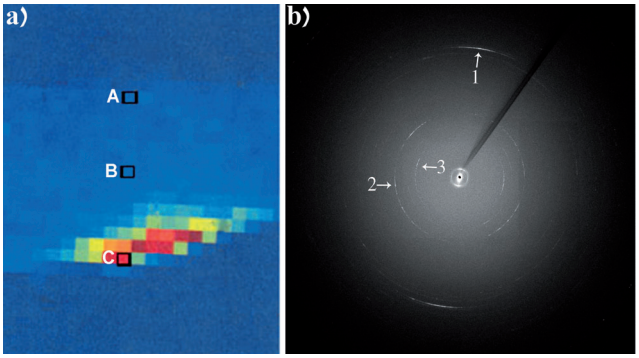

Figure 3. a) X-ray Ca fluorescence map of a cross-section obtained from a Koi scale: area A, within the black box, faces the hypodermis of the fish and area C is near the epidermis of the fish. Brighter colors indicate higher Ca content. b) X-ray diffraction pattern obtained from a fixed Koi scale cross-section. The diffraction pattern was taken from area B in (a): 1 and 2 correspond to the (102) and (012) reflections of anhydrous guanine, whereas 3 corresponds to the (110) reflection of guanine monohydrate.

sets of reflections from anhydrous guanine and hydroxyapatite, a third set of peaks was also detected from areas adjacent to the area of the anhydrous guanine crystals (areas A and B). The peaks at 3.19, 4.09, 4.91, and 9.29 Å, were identified as the $(\bar{3}01)$, (400), (310), and (110) reflections of guanine monohydrate, respectively.

We also analyzed the diffraction patterns of fresh, intact fully hydrated scales at a fixed position on the scale as a function of time. The scales were placed face down on a thin silicon nitride membrane, normal to the source, allowing the beam to pass through the entire thickness of the scale. The spectra were obtained using a beam of 10 μm in diameter. The first diffraction pattern obtained showed a very broad peak at around 1.5–5 Å that corresponded to water, together with the peaks that correspond to the reflections of anhydrous guanine (Figure 4-2; 1 min). As the scale slowly dehydrated, a second

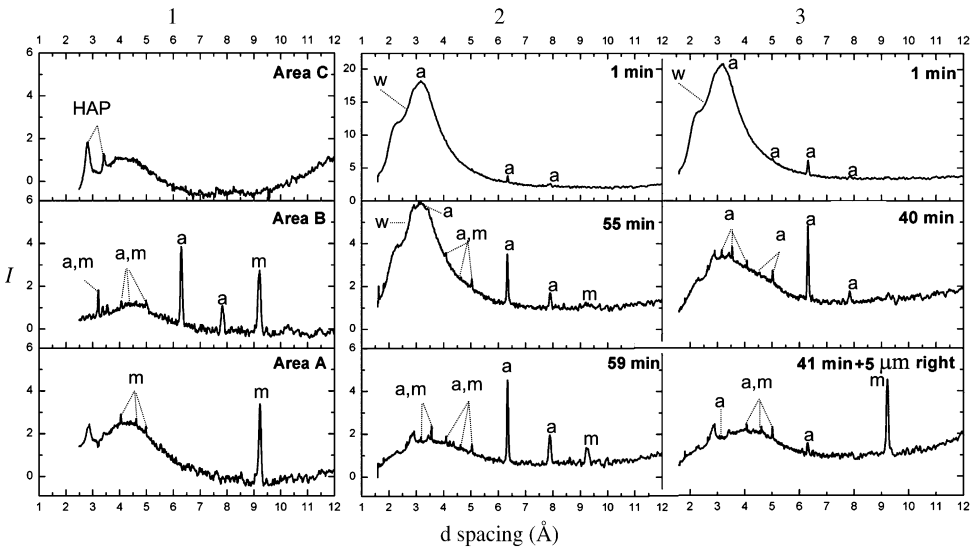

Figure 4. Integrated diffraction patterns. The broad peak of water is marked w = water peak; HAP = hydroxyapatite peaks; a = anhydrous guanine peaks; m = guanine monohydrate peaks. 1) Patterns from different locations in a scale cross-section. A, B, and C correspond to positions A, B, and C in the Ca X-ray fluorescence map (Figure 3). 2) Diffraction patterns collected at a fixed location in a fresh scale after 1, 55, and 59 min of exposure to air. 3) Integrated diffraction patterns collected at a fixed location in a fresh scale after 1 and 40 min, and a diffraction pattern collected after 41 min and 5 μm to the right of the previous location.

phase, corresponding to guanine monohydrate appeared and the broad peak was reduced (Figure 4-2; 55 min and 59 min). The diffraction patterns of guanine monohydrate also have a preferred orientation. The (110) peak is dominant over the $(\bar{3}01)$ diffraction, which should be the strongest peak. The (110) peaks are broad, indicating a disordered material. These phenomena were repeatedly observed using scales from different fish.

One of the scales analyzed showed a different behavior. In the first location examined, the pattern of peaks corresponding to guanine monohydrate was not present, even after the scale was completely dehydrated and the broad peak of water was reduced dramatically (Figure 4-3; 1 min and 40 min). The sets of peaks corresponded only to hydroxyapatite and anhydrous guanine. However, moving the location of the measurement 5 μm to the right of the original location, showed the pattern of guanine monohydrate together with hydroxyapatite and anhydrous guanine (Figure 4-3; 41 min + 5 μm right). This implies that the material that produces the guanine monohydrate is not uniformly distributed, and that the crystals of guanine monohydrate are not derived from the transformation of anhydrous guanine crystals.

As the biogenic crystals are composed solely of anhydrous guanine (Figure 1S), clearly the guanine monohydrate formed from a pre-existing non-diffracting source of guanine, which we refer to as amorphous guanine. We assume that the guanine monohydrate forms because of dehydration of the tissue and/or exposure to the beam. Amorphous guanine should be detectable as a broad peak at low d spacings. Such a broad peak is indeed present in all the spectra (Figure 4). This peak is masked by abundant water scattering in the initial diffraction patterns obtained from specimens just extracted from water. The water peak is reduced as the sample dehydrates, but a broad peak centered at 3.2 Å, persists. In an effort to determine whether the residual peak is indeed, at least in part, due to amorphous material rather than to water, we calculated the ratio between the maximum of the water peak and the background, and compared it to the known ratio for water.[10] The experimental ratio in our measurements was substantially larger than the known ratio for water, supporting the presence of amorphous guanine.

Cryo-SEM image analysis showed the presence of vesicles containing a material denser than the surrounding cytoplasm. Some of the vesicles, usually adjacent to the last formed layer of anhydrous guanine crystals, are elongated in the direction of the ordered crystal stack (Figure 2b), suggesting an intermediate on the way toward crystallization. X-ray diffraction showed that the amorphous phase of guanine is not evenly distributed in the fish scale (Figure 4-3). From these observations we infer, but cannot unequivocally prove, that the source of the amorphous guanine is in the vesicles.

Anhydrous guanine is the stable phase of guanine crystals,[11] whereas pure crystals of guanine monohydrate were only obtained synthetically under extreme conditions.[12] In both phases of guanine, guanine monohydrate and anhydrous guanine, the π–π stacking is the strongest and most dominant interaction in the crystal. In fact, such interactions might be present even in the disordered phase, as a nascent nematic-like phase with short-range order induced by the stacking forces. In the crystals, this would result in a theoretical morphology consisting of prisms elongated in the π–π stacking direction.[3] The crystal structures of both phases are similar. They both have the approximately 3.2 Å spacing characteristic of the π–π stacking as the dominant peak in the theoretical spectrum. In biogenic anhydrous guanine, the crystals are induced by the cells to grow as {102} plates, developed in the plane perpendicular to the [102] π–π stacking direction. The common orientation of the crystal platelets in the scales, namely parallel to the scale direction, causes a strong orientation effect on the (102) reflection, such that when the scale is observed face-on the reflection is very weak. The guanine monohydrate diffraction pattern also shows a preferred orientation, similar to the anhydrous phase. Specifically, the (110) reflection is much stronger than the strongest expected reflection, $(\bar{3}01)$, corresponding to the stacking direction in the monohydrate phase. It is conceivable that the

same constraints that induce the platelet anhydrous guanine morphology are operative also for the induced formation of guanine monohydrate, resulting in a $(\bar{3}01)$ platelet morphology.

The scale is composed of a dense and rigid mineralized tissue (mineralized collagen matrix) and a soft hydrated cellular tissue. Dehydrating the scale can thus cause stretching of the softer tissue, which in turn will cause stretching of the vesicles. Such a process may facilitate crystallization of the guanine molecules, together with the trapped water inside the vesicles, to form oriented crystals of guanine monohydrate. In many organisms that form mineralized skeletal tissues, mineral-containing vesicles are found in the cells responsible for producing this mineralized tissue. Examples are mollusks, crustaceans, and echinoderms.[13] The mineral phases in many of those vesicles are highly disordered. Vertebrate cells responsible for bone mineralization were recently found to contain vesicles with amorphous calcium phosphate (ACP).[14] Thus the presence of amorphous guanine in vesicles inside cells, responsible for the anhydrous guanine crystal formation, would be consistent with many other observations.

In conclusion, herein we showed that a disordered guanine phase is a precursor of crystalline anhydrous guanine in the scales of Koi fish. This is possibly the first evidence of the use of an amorphous precursor phase in vivo in a biogenic organic crystal.

Received: July 6, 2012
Published online: September 5, 2012

Keywords: amorphous materials · biogenic guanine crystals · photonic crystals · structural colors · X-ray diffraction

[1] P. Herring, *Comp. Biochem. Physiol. Part A* **1994**, *109*, 513 – 546.
[2] a) E. J. Denton, J. A. C. Nicol, *J. Mar. Biol. Assoc. U.K.* **1965**, *45*, 683 – 703; b) E. J. Denton, *Philos. Trans. R. Soc. London Ser. B* **1970**, *258*, 285 – 313; c) E. J. Denton, M. F. Land, *Philos. Trans. R. Soc. London Ser. B* **1971**, *178*, 43 – 61; d) M. F. Land, *Prog. Biophys. Mol. Biol.* **1972**, *24*, 75 – 106.
[3] A. Levy-Lior, B. Pokroy, B. Levavi-Sivan, L. Leiserowitz, S. Weiner, L. Addadi, *Cryst. Growth Des.* **2008**, *8*, 507 – 511.
[4] a) A. R. Parker, D. R. McKenzie, M. C. J. Large, *J. Exp. Biol.* **1998**, *201*, 1307 – 1313; b) A. R. Parker, *J. Opt. A* **2000**, *2*, R15 – R28; c) P. Vukusic, J. R. Sambles, C. R. Lawrence, R. J. Wootton, *Nature* **2001**, *410*, 36 – 36; d) S. Kinoshita, S. Yoshioka, *ChemPhysChem* **2005**, *6*, 1442 – 1459; e) S. Kinoshita, S. Yoshioka, J. Miyazaki, *Rep. Prog. Phys.* **2008**, *71*, 076401; f) A. F. Huxley, *J. Exp. Biol.* **1968**, *48*, 227 – 245.
[5] a) S. Weiner, L. Addadi, *Annu. Rev. Mater. Res.* **2011**, *41*, 21 – 40; b) K. M. Towe, H. A. Lowenstam, *J. Ultrastruct. Res.* **1967**, *17*, 1 – 13; c) A. Al-Sawalmih, C. Li, S. Siegel, H. Fabritius, S. Yi, D. Raabe, P. Fratzl, O. Paris, *Adv. Funct. Mater.* **2008**, *18*, 3307 – 3314.
[6] a) P. Hartman, W. G. Perdok, *Acta Crystallogr.* **1955**, *8*, 49 – 52; b) I. Weissbuch, L. Addadi, L. Leiserowitz, *Science* **1991**, *253*, 637 – 645.
[7] a) R. J. Davey, N. Blagden, G. D. Potts, R. Docherty, *J. Am. Chem. Soc.* **1997**, *119*, 1767 – 1772; b) R. J. Davey, N. Blagden, S. Righini, H. Alison, M. J. Quayle, S. Fuller, *Cryst. Growth Des.* **2001**, *1*, 59 – 65.
[8] A. Levy-Lior, E. Shimoni, O. Schwartz, E. Gavish-Regev, D. Oron, G. Oxford, S. Weiner, L. Addadi, *Adv. Funct. Mater.* **2010**, *20*, 320 – 329.
[9] D. L. Fox, *Animal biochromes and structural colours; physical, chemical, distributional & physiological features of coloured bodies in the animal world*, University Press, Cambridge Eng., **1953**.
[10] G. Hura, J. M. Sorenson, R. M. Glaeser, T. Head-Gordon, *J. Chem. Phys.* **2000**, *113*, 9140 – 9148.
[11] K. Guille, W. Clegg, *Acta Crystallogr. C* **2006**, *62*, O515 – O517.
[12] U. Thewalt, C. E. Bugg, R. E. Marsh, *Acta Crystallogr. Sect. B* **1971**, *27*, 2358 – 2363.
[13] a) B. E. Brown, *Bio. Rev.* **1982**, *57*, 621 – 667; b) E. Beniash, L. Addadi, S. Weiner, *J. Struct. Biol.* **1999**, *125*, 50 – 62.
[14] a) J. Mahamid, A. Sharir, L. Addadi, S. Weiner, *Proc. Natl. Acad. Sci. USA* **2008**, *105*, 12748 – 12753; b) J. Mahamid, B. Aichmayer, E. Shimoni, R. Ziblat, C. Li, S. Siegel, O. Paris, P. Fratzl, S. Weiner, L. Addadi, *Proc. Natl. Acad. Sci. USA* **2010**, *107*, 6316 – 6321; c) J. Mahamid, A. Sharir, D. Gur, E. Zelzer, L. Addadi, S. Weiner, *J. Struct. Biol.* **2011**, *174*, 527 – 535.

